Origin and Enhancement of Hole-Induced Ferromagnetism in First-Row d^0 Semiconductors

Haowei Peng,[1] H. J. Xiang,[2] Su-Huai Wei,[2,*] Shu-Shen Li,[1] Jian-Bai Xia,[1] and Jingbo Li[1,†]

[1]*State Key Laboratory for Superlattices and Microstructures, Institute of Semiconductors, Chinese Academy of Sciences, P. O. Box 912, Beijing 100083, People's Republic of China*

[2]*National Renewable Energy Laboratory, Golden, Colorado 80401*

(Received 23 October 2008; revised manuscript received 24 October 2008; published 5 January 2009)

The origin of ferromagnetism in d^0 semiconductors is studied using first-principles methods with ZnO as a prototype material. We show that the presence of spontaneous magnetization in nitrides and oxides with sufficient holes is an intrinsic property of these first-row d^0 semiconductors and can be attributed to the localized nature of the $2p$ states of O and N. We find that acceptor doping, especially doping at the anion site, can enhance the ferromagnetism with much smaller threshold hole concentrations. The quantum confinement effect also reduces the critical hole concentration to induce ferromagnetism in ZnO nanowires. The characteristic nonmonotonic spin couplings in these systems are explained in terms of the band coupling model.

DOI: 10.1103/PhysRevLett.102.017201 PACS numbers: 75.10.Lp, 71.20.Nr, 75.75.+a

In the field of spintronics, ferromagnetic semiconductors have special advantages because of their easy integration into semiconductor devices [1]. Most of the previous studies have been focused on dilute magnetic semiconductors (DMS), in which the magnetic moments are introduced by doping magnetic $3d^n$ transition-metal (TM) ions into semiconductors [2–4]. Recently, however, unexpected high-temperature ferromagnetism has been observed in a series of materials, which do not contain ions with partially filled d or f bands [5–14]. This type of "d^0 ferromagnetism" [15] provides a new opportunity for searching high-temperature spintronic materials. However, it also provides a challenge to understand the origin of the magnetism in these materials, i.e., whether the observed magnetism is an intrinsic property of the host material or it is an extrinsic property depending sensitively on the type of dopant used to induce the magnetization. To improve the physical properties of these materials, it is important to understand the mechanism of such phenomena, and design new approaches to enhance the magnetic interactions.

In this Letter, the so-called "d^0 ferromagnetism" is investigated via first-principles calculations, with ZnO as the main prototype material. We show that the hole-induced magnetization in these materials is intrinsic for first-row nitrides and oxides. It is caused by large spin-exchange interaction at N, O, and other first-row element sites and due to large density of states (DOS) in the ionic nitride and oxide compounds near the valence band maximum (VBM). Moreover, sufficient hole carrier density is required to move the Fermi surface away from the VBM so that magnetization can be sustained. Based on this understanding, we show that the magnetization can be enhanced by doping the nitrides or oxides using localized acceptors or using the quantum confinement effect to localize the hole states.

The calculations were performed using the all-electron projector augmented wave method [16] encoded in the plane-wave basis Vienna *ab initio* simulation package (VASP) [17], using the density functional theory with generalized gradient approximations (GGA) [18]. Convergence with respect to the plane-wave cutoff energy and k-point sampling has been carefully checked. For relaxed structures, the atomic forces are less than 0.01 eV/Å. Holes are injected by removing electrons from the system and using a jellium background to maintain charge neutrality. The defect calculation is performed using a 128-atom $4 \times 4 \times 2$ wurtzite supercell.

Origin of spin polarization in d^0 semiconductors.—To understand this issue, we calculate the total magnetic moments as a function of injected holes for zinc blende ZnO, ZnS, GaN, and GaP, comparatively. Meanwhile, polarization energy, which is the total energy difference between the spin-polarized and nonspin-polarized phases, is calculated to check the stability of the magnetization. Similar calculations have been done for wurtzite cells and the results are very similar. The results for ZnO are plotted in Fig. 1. We find that for small hole concentration m_h, the

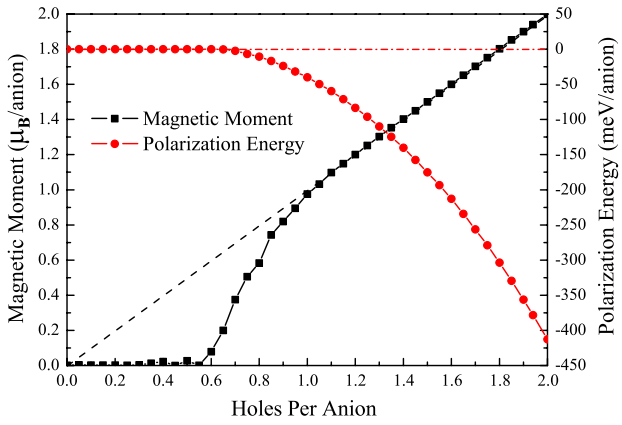

FIG. 1 (color online). Magnetic moments and polarization energy of hole-injected ZnO in zinc blende structure.

system continues to be nonmagnetic, which is true for ZnS and GaP even for high hole density. However, for large hole concentration, ZnO and GaN become spin polarized. The critical hole concentration is 0.60 per anion for ZnO and 0.65 per anion for GaN, corresponding to 2.67×10^{22} cm^{-3} and 2.77×10^{22} cm^{-3}, respectively. As shown in Fig. 1, the turn-on of the magnetization is quite sharp. At one hole per cell, the net magnetic moments are 0.97 and $0.62\mu_B$ per anion for ZnO and GaN, respectively.

To understand this behavior, we notice that in ZnO and GaN the magnetic moments are contributed mainly by the states at the top of the valence band, which has mostly anion p character. In the band-picture model, spontaneous ferromagnetism occurs when the relative gain in exchange interaction is larger than the loss in kinetic energy, i.e., when it satisfies the "Stoner Criterion": $D(E_f)J > 1$, where $D(E_f)$ is the DOS at the Fermi energy E_f, and J denotes the strength of the exchange interaction [19]. Our calculated results can easily be explained by this simple model. The reasons that oxides and nitride can be spin-polarized by injecting holes are as follows. (i) First-row elements N and O have very large exchange interaction J for the $2p$ orbitals compared to the P and S $3p$ orbitals. Table I shows the calculated spin-exchange splitting energy $\epsilon\downarrow - \epsilon\uparrow$ for N, O, P, and S valence p orbitals, as well as for Mn d orbitals for $M = 2\mu_B$. The exchange interaction and the energy gain from the nonspin-polarized phase are proportional to the splitting. We find that the splitting energy for the $2p$ orbitals is about twice as large as for the $3p$ orbitals. It is even larger than that for the Mn $3d$ orbitals with the same moment. (ii) For oxides and nitrides, the top of the valence band is quite flat with large effective masses. This is because due to the high ionicity, the top of the valence band for oxides and nitrides is mostly anion atomic p-like, thus very localized. Figure 2 plots the radial charge distribution $4\pi r^2\rho(r)$ for the N and O $2p$ and P and S $3p$ atomic orbitals. We also plot the $3d$ atomic orbital in Mn, which is a typical magnetic element. From the comparison, we find that the $2p$ atomic orbitals have a similar degree of spatial localization as the $3d$ atomic orbital, whereas the $3p$ atomic orbitals are much more delocalized. Because the density of states $D(E_f)$ is proportional to $m^{3/2}\sqrt{E_{\mathrm{VBM}} - E_f}$ when holes are introduced, magnetization can be sustained only in compounds with large effective mass m such as oxides.

The dependence on the E_f for the density of states also explains why sufficient hole density is needed to turn on the magnetization. This is because when hole density approximates zero, the Fermi level lies just at the VBM, and the $D(E_f)$ is close to zero, resulting in no magnetic moment because $D(E_f)J < 1$. When there are more holes, the Fermi level moves into the valence band and the DOS at the Fermi level increases, proportional to $\sqrt{E_{\mathrm{VBM}} - E_f}$. When the hole concentration becomes large enough so that $D(E_f)J > 1$, the system becomes spin polarized. However, our calculations and discussion above show that it is not easy to obtain magnetic moment and ferromagnetism only by injecting holes uniformly into these systems. The reason is because for oxide and nitride semiconductors, p-type doping with a very high hole concentration is difficult, if not impossible, to achieve because they have very low valence band energies [20]. In the following, we will discuss several approaches to enhance the magnetization through acceptor doping or quantum confinement. This is because by acceptor doping or quantum confinement, we can increase *local* hole concentration at the anion site so that the local DOS at the Fermi level and the exchange interaction are large; thus, magnetization can be achieved with a reasonable amount of global hole concentration.

Cation-site doping-induced magnetization in ZnO: V_{Zn}.—We first consider cation vacancy doping. When a neutral Zn atom is removed, two holes are introduced with the hole wave function distributed mostly on the four neighboring tetrahedral oxygen sites. The resulting total magnetic moment for the unrelaxed system is $2.00\mu_B$, equal to the number of holes. The local magnetic moment is $0.25\mu_B$ at each of the neighboring O sites, and $0.02\mu_B$ on each of the 12 hcp nearest Zn atom sites. The small spin density at the cation sites, as well as at the vacancy site, is consistent with the fact that the defect level is derived from the top of the valence band, which consists mostly of anion p orbitals. However, in this case, the hole wave function is not very localized, and we find that the local magnetic moment at the seventh nearest neighbor (NN) oxygen site (about 5.06 Å from the defect center) is $0.03\mu_B$, i.e., not negligible. This is consistent with the fact that the V_{Zn} energy level is not very deep, at about 0.14 eV above the

TABLE I. Calculated spin-exchange splitting energy $\epsilon\downarrow - \epsilon\uparrow$ for N, O, P, and S valence p orbitals, as well as for Mn d orbitals, for $M = 2\mu_B$.

Orbitals	N, $2p$	O, $2p$	P, $3p$	S, $3p$	Mn, $3d$
$\epsilon\downarrow - \epsilon\uparrow$ (eV)	2.57	2.82	1.32	1.42	1.62

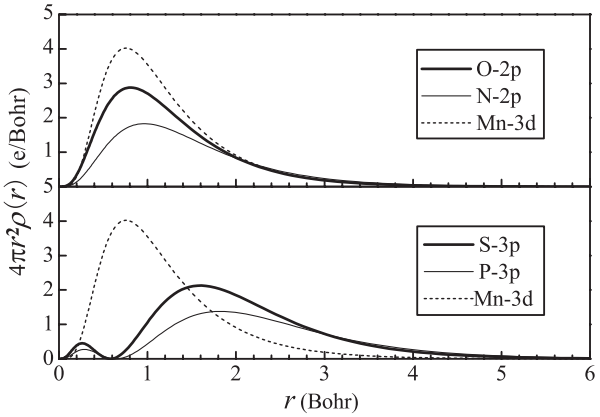

FIG. 2. Radial charge distribution, $4\pi r^2\rho(r)$, for N, O, P, and S valence p orbitals as well as for Mn d orbitals.

VBM. However, after full atomic relaxation, the total magnetic moment decreases to $1.50\mu_B$, with most of the loss taking place in the NN oxygen sites. We find that this decrease is due to the large outward relaxation of the NN oxygen atoms. They move outward by about 10%, which makes the defect level shallower and wave function more delocalized, resulting in a smaller DOS at the Fermi level, and thus, a smaller spin-exchange splitting. The spin-polarization energy is found to be 40 meV for an isolated V_{Zn} defect.

Anion-site doping-induced magnetization in ZnO: C_O.— The discussion above shows that magnetization through cation-site doping is achievable, but not very efficient because the holes are distributed into several neighboring anion sites. Therefore, it will be more effective if the hole doping occurs directly at the anion site, such as C substitution on the O site (C_O). In this case, the C $2p$ orbital is localized just like the O $2p$ orbital, and each C_O defect creates two holes, just as V_{Zn} can. We find that for C_O, the majority spin defect level is fully occupied, whereas the minority spin level is only partially occupied, resulting in a total magnetic moment of $2.00\mu_B$. $0.60\mu_B$ is located at the C_O site, $0.1\mu_B$ on each of the four NN Zn sites, $0.034\mu_B$ on each of the 12 hcp NN O sites, and the rest are mostly distributed in the interstitial spaces around these atoms. This indicates that compared to V_{Zn}, the defect wave function of C_O is more localized, which is consistent with the fact that the C_O defect level at 0.56 eV above the VBM is also deeper. The localized C_O results in a large spin-exchange splitting and a large spin-polarization energy of 360 meV per defect, much larger than that for the V_{Zn} doped system. This confirmed our expectation that direct hole doping at the anion site is more effective for localizing the hole and sustaining the magnetic moment.

To investigate the magnetic coupling between these hole-induced moments, we put two defects in the 128-atom supercell. We first consider two configurations: (a) the defects are in second hcp NN positions separated by a distance of about 4.63 Å; and (b) the defects are in 11th hcp NN positions separated by a distance of about 8.44 Å, the largest possible distance within the supercell. The energy difference between the ferromagnetic (FM) and antiferromagnetic (AFM) phases, ΔE, and the total magnetic moment of the FM phase are shown in Table II. First, we can see that for both configurations and both dopants, the FM state has a lower energy than the AFM state. Second, we can see that for V_{Zn} doping, the energy difference between the AFM state and the FM state and the total magnetic moment becomes smaller when two vacancies are closer to each other. In contrast, for C_O doping, the energy difference is larger in the second NN sites than in the 11th NN sites, and the total magnetic moment is the same in the two configurations.

The stabilization of the FM phase observed for these systems can be understood using the phenomenological band-coupling model [21] (see Fig. 3). For the isolated defect C_O, the majority spin is fully occupied, whereas the minority spin is only partially occupied. In the FM phase, the $2p$ states with the same spin can couple to each other, forming bonding and antibonding states. The increased occupation of the spin-down bonding states stabilizes the FM phase [Fig. 3(a)]. The AFM phase is stabilized by the superexchange interaction between the occupied majority spin state on one site and the partially occupied minority spin state on the other site. The gain in energy is usually larger in the FM state than in the AFM state due to the second-order nature of the superexchange interaction [Fig. 3(c)], so the system is more stable in FM. The interaction increases as the defect-defect distance decreases; therefore, as long as there is no overlap between the majority occupied and minority unoccupied states, ΔE will increase (Table II). However, as the two C_O defects become very close (hcp NN with a separation of about 3.28 Å), the total moment decreases from $4.00\mu_B$ to $2.00\mu_B$, and the system can even be more stable in the AFM phase. This is because in this case, the large coupling broadens the spin-up and spin-down band widths, causing a charge transfer from the majority spin state to the minority spin state, thus reducing the local moment and exchange splitting [Fig. 3(b)]. The reduced exchange splitting stabilizes the AFM phase, and can cause it to be the ground state. This agrees with the experiment [11] that revealed a decreasing magnetic moment per carbon as the carbon concentration increases, because the defect bands broaden as the C concentration increases.

For V_{Zn}, the situation is similar to that found in C_O, except the V_{Zn} defect wave function is more delocalized and the defect band widths are larger. This results in a larger overlap of the spin majority band with the minority band, and thus, a charge transfer between the two spin channels even when the defect separation is relatively large. As a consequence, the total moment is reduced when the two V_{Zn} are next NN, which leads to a reduced energy difference ΔE between the AFM and FM states (Table II). Further reduction of the distance between the V_{Zn} can even make the magnetic moment disappear. This

TABLE II. The energy difference between the ferromagnetic (FM) and antiferromagnetic (AFM) phases $\Delta E = E^{AFM} - E^{FM}$, and the total magnetic moment for the FM phase.

	Configuration a ($d = 4.63$ Å)		Configuration b ($d = 8.44$ Å)	
	ΔE (meV)	M (μ_B)	ΔE (meV)	M (μ_B)
V_{Zn}	16	3.25	32	3.50
C_O	35	4.00	12	4.00

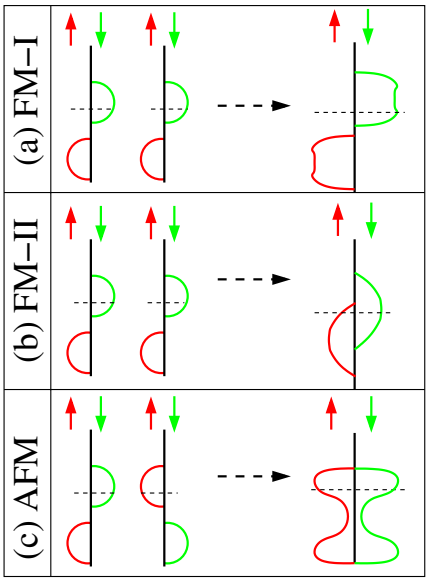

FIG. 3 (color online). Schematic illustration of the possible coupling in "d^0 systems." The DOS in the majority and minority spin channels are plotted in red and green, respectively. The dashed line denotes the Fermi level. The left side shows the DOS for two isolated defects, and the right side is the final state after the coupling for the whole system. FM-I and FM-II correspond to relatively long and short interdefect distances.

explains the different behavior between V_{Zn} and C_O. So, in the "d^0 systems," the ferromagnetism has a maximum stability at a critical doping concentration, which is proportional to the degree of the localization of the magnetic moment. A similar situation was found in Cu-doped GaN systems [22].

Quantum confinement effects induced magnetization in ZnO nanowires.—As discussed above, doping-induced hole localization can enhance the magnetization. Here, we show that the quantum confinement effect can also be used to enhance hole-induced magnetization. To demonstrate this, we try to inject holes into a [0001] ZnO nanowire with a diameter of 1 nm. The surface dangling bonds have been passivated by pseudohydrogen atoms. For a parabolic band in one-dimensional systems, the DOS has a singularity near the band edge: $D \propto 1/\sqrt{E - E_0}$. Thus, it is expected that even a small number of holes can lead to spin-polarization in semiconducting nanowires. Indeed, our calculations show that the critical hole concentration needed to induce ferromagnetism is less than 1/8 of that needed in bulk materials.

Recently, Garcia *et al.* found a room-temperature ferromagneticlike behavior [12] when the ZnO nanoparticle is capped with dodecanethiol, which bonds to the particle surface through the S atom. Similar to our calculations on a ZnO nanowire, this could be attributed to the holes induced by charge transfer between the Zn and S.

In summary, we studied the origin of "d^0 ferromagnetism" with ZnO as a prototype material. We showed that hole-induced magnetization in oxides, nitrides and diamond are an intrinsic host property when enough homogeneous holes are injected into the system. We further demonstrated that localization of the holes by dopants and quantum confinement effect can reduce the critical hole concentration for stabilizing magnetization. The nonmonotonic spin coupling in this system is explained by considering band broadening as a function of defect-defect separation.

J. Li gratefully acknowledges financial support from the "One-hundred Talents Plan" of the Chinese Academy of Sciences. This work was supported by the National Basic Research Program of China (973 Program) Grant No. G2009CB929300 and the National Natural Science Foundation of China under Grants No. 60521001 and No. 60776061. The work at NREL is supported by the U.S. DOE under Contract No. DE-AC36-08GO28308.

*Suhuai_Wei@nrel.gov
†jbli@semi.ac.cn

[1] S. A. Wolf *et al.*, Science **294**, 1488 (2001).
[2] H. Ohno, Science **281**, 951 (1998).
[3] T. Dietl, H. Ohno, F. Matsukura, J. Cibert, and D. Ferrand, Science **287**, 1019 (2000).
[4] T. Jungwirth, J. Sinova, J. Mašek, J. Kušera, and A. H. MacDonald, Rev. Mod. Phys. **78**, 809 (2006).
[5] I. S. Elfimov, S. Yunoki, and G. A. Sawatzky, Phys. Rev. Lett. **89**, 216403 (2002).
[6] R. Monnier and B. Delley, Phys. Rev. Lett. **87**, 157204 (2001).
[7] M. Venkatesan, C. B. Fitzgerald, and J. M. D. Coey, Nature (London) **430**, 630 (2004).
[8] J. M. D. Coey, M. Venkatesan, P. Stamenov, C. B. Fitzgerald, and L. S. Dorneles, Phys. Rev. B **72**, 024450 (2005).
[9] C. Das Pemmaraju and S. Sanvito, Phys. Rev. Lett. **94**, 217205 (2005).
[10] N. H. Hong, J. Sakai, N. Poirot, and V. Brizé, Phys. Rev. B **73**, 132404 (2006).
[11] H. Pan *et al.*, Phys. Rev. Lett. **99**, 127201 (2007).
[12] M. A. Garcia *et al.*, Nano Lett. **7**, 1489 (2007).
[13] K. Nomura and A. H. MacDonald, Phys. Rev. Lett. **96**, 256602 (2006).
[14] H. Ohldag *et al.*, Phys. Rev. Lett. **98**, 187204 (2007).
[15] J. M. D. Coey, Solid State Sci. **7**, 660 (2005).
[16] G. Kresse and D. Joubert, Phys. Rev. B **59**, 1758 (1999).
[17] G. Kresse and D. Joubert, Comput. Mater. Sci. **6**, 15 (1996).
[18] J. P. Perdew and Y. Wang, Phys. Rev. B **33**, 8800 (1986).
[19] E. C. Stoner, Proc. R. Soc. A **165**, 372 (1938); **169**, 339 (1939).
[20] S.-H. Wei, Comput. Mater. Sci. **30**, 337 (2004).
[21] G. M. Dalpian, S.-H. Wei, X. G. Gong, A. J. R. Da Silva, and A. Fazzio, Solid State Commun. **138**, 353 (2006).
[22] H. J. Xiang and S.-H. Wei, Nano Lett. **8**, 1825 (2008).